Effect of Ag or Sb addition on the thermoelectric properties of PbTe

H. S. Dow,[1] M. W. Oh,[2,a)] B. S. Kim,[2] S. D. Park,[2] B. K. Min,[2] H. W. Lee,[2] and D. M. Wee[1]
[1]*Department of Materials Science and Engineering, KAIST, Daejeon 305-701, South Korea*
[2]*Advanced Material and Application Research Division, Korea Electrotechnology Research Institute, Changwon 641-120, South Korea*

(Received 7 September 2010; accepted 17 October 2010; published online 6 December 2010)

In this study, the effect of Ag or Sb addition on the thermoelectric properties of PbTe including the Seebeck coefficient, the electrical resistivity, and the thermal conductivity, was studied in the temperature range from 323 to 723 K. The major carriers in the Ag-doped and the Sb-doped PbTe are holes and electrons, respectively. A degenerate semiconductor behavior in the electrical transport properties was observed in the Ag-doped, whereas the semi-metallic in the Sb-doped. It was suggested from the results of the Hall effect measurement and the Seebeck coefficient that the effective mass was significantly altered by the Sb-doping. The maximum dimensionless figure of merit, *ZT*, of $Pb_{1-x}Ag_xTe$ and $Pb_{1-x}Sb_xTe$ (x=0.1) alloys showed 0.27 and 0.62 at 723 K, respectively. Based on the analysis of the Seebeck coefficient of the Ag or the Sb-doped PbTe, the interaction between Ag and Sb in PbTe, as expected in the $AgPb_mSbTe_{m+2}$ (LAST-m), may be supposed. © *2010 American Institute of Physics*. [doi:10.1063/1.3517088]

I. INTRODUCTION

Thermoelectric devices have attracted much interest because they can generate electrical power from temperature difference which can be easily obtained from the waste heat sources.[1,2] The efficiencies of thermoelectric power generation as well as thermoelectric refrigeration in thermoelectric devices can be described in terms of the dimensionless figure of merit (*ZT*) which can be expressed as, $ZT=S^2T/\rho\kappa$ where *S* is the Seebeck coefficient, ρ is the electrical resistivity, κ is the thermal conductivity, and *T* is the absolute temperature.[1] Thus the good thermoelectric performance requires a large value for *S* and small value for ρ and κ.

Among the developed many thermoelectric materials, lead telluride (PbTe) has been presented as a highly attractive thermoelectric material. PbTe and its alloys have optimum thermoelectric materials at the temperature of approximately 700 K.[3] Concentrated research has been performed to improve the thermoelectric performance of the PbTe alloys; such research was based on the substitution and addition of other elements for the modification of the thermal conductivity and the carrier concentration of the PbTe alloys.[4–7] Hsu *et al.*[8] have recently reported that the $AgPb_mSbTe_{m+2}$ (LAST-m, m=10, and m=18) alloys showed n-type properties and the outstanding *ZT*=2.2 at 800 K, which was highest than any other results in previous PbTe research. In addition, Zhou *et al.*[9] reported that the off-stoichiometric LAST-18 alloys showed *ZT*=1.5 at 700 K. Notwithstanding these previous outstanding results, the effects of Ag and Sb co-doping on the thermoelectric properties for the PbTe alloys were unclear.

To understand the effect of the co-doping, the investigation of the role of single element doping of Ag or Sb on the thermoelectric properties of PbTe may be helpful. In this work, a comprehensive investigation of the $Pb_{1-x}Ag_xTe$ and the $Pb_{1-x}Sb_xTe$ alloys (x=0.02, 0.04, 0.06, 0.08, and 0.1) on the thermoelectric properties was performed in the temperature range from 323 to 723 K. Several works on the thermoelectric properties of the Ag or the Sb-doped PbTe exist already.[10–13] However they couldn't be compared with the thermoelectric properties of the LAST-m alloys because the thermoelectric properties of LAST-m is highly dependent of the fabrication condition and procedure.[14–16] To investigate more systematically, we may need to perform same fabrication procedure used in the LAST-m alloys. Thus, we followed identical procedure used in our previous work on the LAST-m compounds.[17] In addition to the microstructure, the thermoelectric properties including the Seebeck coefficient, the electrical resistivity, and the thermal conductivity were investigated at elevated temperatures. The effect of the co-doping on the thermoelectric properties was also discussed.

II. EXPERIMENTAL DETAILS

The fabrication procedures used in Ref. 17 were followed here to compare the results. The samples with the nominal composition of the $Pb_{1-x}Ag_xTe$ and the $Pb_{1-x}Sb_xTe$ alloys (x=0.02, 0.04, 0.06, 0.08, and 0.1) were prepared. Raw elements of Pb, Te, Ag, and Sb were cleaned with HNO_3, HCl, acetone, and ethanol in series for 10 min via ultrasonic cleaning. The weighed elements were inserted into the quartz tube and evacuated to 10^{-5} Torr. After inserting Ar gas, the tubes were sealed to prevent oxidation during the melting process. The sealed quartz tube including the raw elements was placed in a rocking furnace at 1223 K during 10 h and then cooled in the rocking furnace. The obtained alloys were cut into rectangular pieces ($3\times3\times10$ mm^3) for the thermoelectric measurement and cylinder pieces (12.7 mm in diameter and 1 mm in thickness) for the thermal diffusivity measurement.

a)Electronic mail: minwookoh@keri.re.kr.

The analysis of the phase of the $Pb_{1-x}Ag_xTe$ and the $Pb_{1-x}Sb_xTe$ ternary alloys were carried out using x-ray diffraction [(XRD) Rigaku D/max-rc(12kw)] with Cu $K\alpha$. The analysis of the morphology and the element composition of the $Pb_{1-x}Ag_xTe$ and the $Pb_{1-x}Sb_xTe$ alloys were carried out using scanning electron microscopy (SEM, Hitachi S-4800). The densities of the melted alloys were measured by the Archimedes method. A differential scanning calorimeter (NETZSCH, DSC 404C) was used for the measurement of the heat capacity. The thermoelectric properties were analyzed by ZEM-3 (ULVAC-RIKO, Japan) for the measurement of the Seebeck coefficient and the electrical resistivity. The thermal conductivity of the $Pb_{1-x}Ag_xTe$ and the $Pb_{1-x}Sb_xTe$ alloys was calculated from the results of the density (d), the heat capacity (C_P), and the thermal diffusivity (α), using this equation: $\kappa = \alpha C_P d$. Thermal diffusivity was measured by the laser flash method (NETZSCH, LFA-457). The Hall effect measurements was conducted in a magnet of 0.55 T for analysis of the carrier concentration and mobility.

III. RESULTS AND DISCUSSION

Figure 1 shows the patterns of the XRD for $Pb_{1-x}Ag_xTe$ and $Pb_{1-x}Sb_xTe$. The major phases are the poly crystalline PbTe compound in a NaCl structure. The measured density values of all samples are approximately 8.1 g/cm^3, which is well above 95% of the theoretical density. The relative densities of the ternary compounds are similar with those of the LAST-m compounds fabricated with the same procedure.[17] The second phases are apparently observed in both $Pb_{1-x}Ag_xTe$ and $Pb_{1-x}Sb_xTe$ alloys at a higher content of the dopants. The second phases are identified as Ag_5Te_3 and Sb_2Te_3 in $Pb_{1-x}Ag_xTe$ and $Pb_{1-x}Sb_xTe$, respectively. The lattice parameters of $Pb_{1-x}Ag_xTe$ and $Pb_{1-x}Sb_xTe$ are calculated and plotted in Fig. 2 as a function of the composition. Because the ionic radii of Ag (~1.60 Å) and Sb (~1.45 Å) are smaller than that of Pb (~1.80 Å), the lattice parameters of the doped samples are reduced. Moreover the lattice parameters of the Sb-doped samples are smaller than those of the Ag-doped, because the ionic radius of Sb is smaller than that of Ag. The reduction in the lattice parameters in both samples means that the doping elements are substituted for Pb. If Sb or Ag is fully substituted for Pb in the whole composition range, the lattice parameters should be monotonically decreased with increasing the composition, according to Vegard's law. However it is hard to say the parameters are changed as mentioned before, which may imply the dopant elements are not substituted for Pb in the whole composition range but in the small composition range. The solubility limit of Sb in PbTe seems to be larger than that of Ag, because the variation in the lattice parameters with the composition is limited in the Ag-doped compounds. It is known that the solubility limit of Ag and Sb for PbTe are about $x = 0.006-0.007$ and 0.02 in $Pb_{1-x}M_xTe$, respectively, which supports the observation here.[18–20]

Figure 3 shows the SEM images of the $Pb_{1-x}Ag_xTe$ and the $Pb_{1-x}Sb_xTe$ ($x = 0.02$ and 0.1) alloys. The second phases of Ag_5Te_3 are observed in all composition of $Pb_{1-x}Ag_xTe$ ($0.02 < x < 0.1$) and Sb_2Te_3 are also placed in all

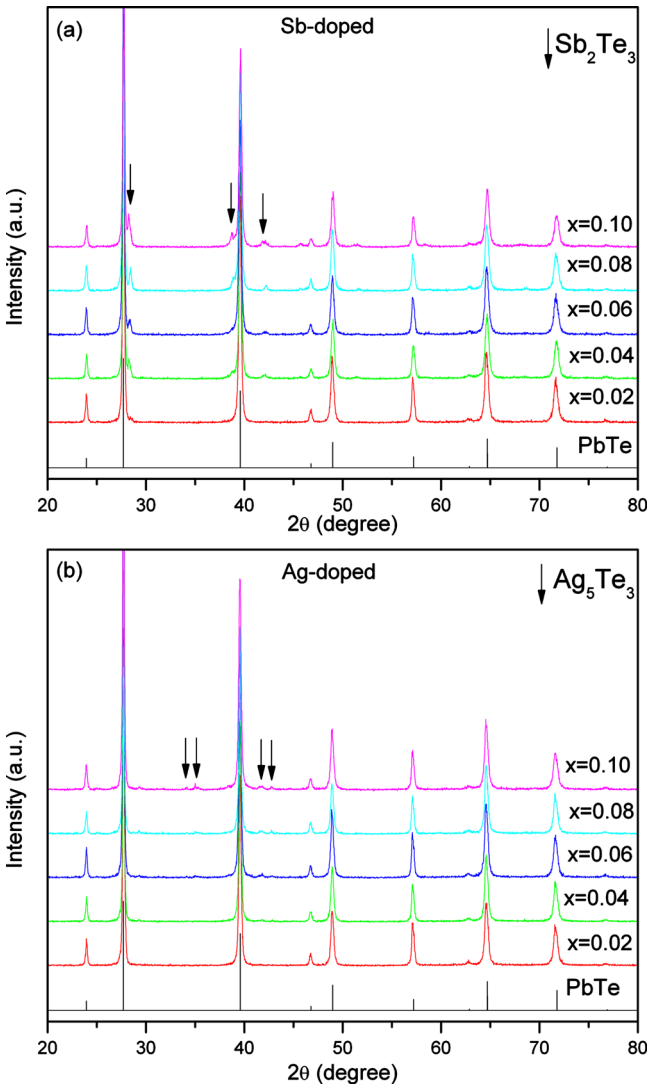

FIG. 1. (Color online) XRD patterns of (a) the $Pb_{1-x}Sb_xTe$ and (b) the $Pb_{1-x}Ag_xTe$ ($x = 0.02$, 0.04, 0.06, 0.08, and 0.1) alloys. Reference data (PDF No. 78-1904) for cubic PbTe is included.

$Pb_{1-x}Sb_xTe$. It may be concluded that the second phases are not observed in the XRD analysis due to its small volume fraction. The energy dispersive x-ray spectrum analysis is shown in Table I. It is hard to detect Sb and Ag in the matrix

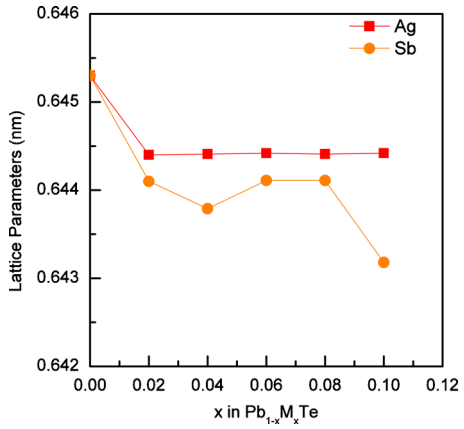

FIG. 2. (Color online) Lattice parameters of $Pb_{1-x}M_xTe$ (M: Ag or Sb) as a function of composition.

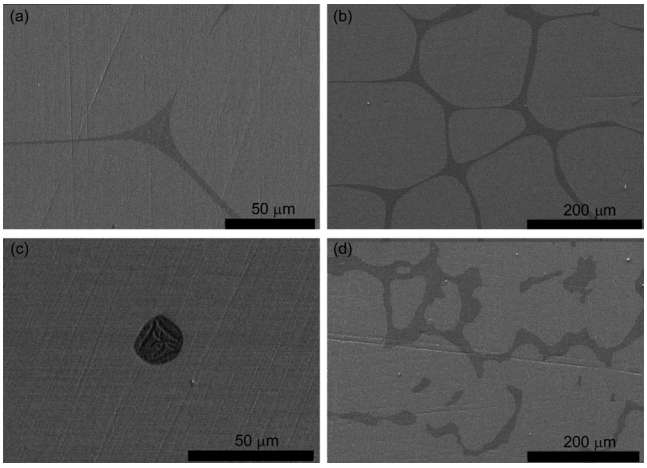

FIG. 3. SEM images of the $Pb_{1-x}Ag_xTe$ [(a) and (b)] and the $Pb_{1-x}Sb_xTe$ [(c) and (d)] alloys. Images of (a) and (c) are for x=0.02, while (b) and (d) are for x=0.1.

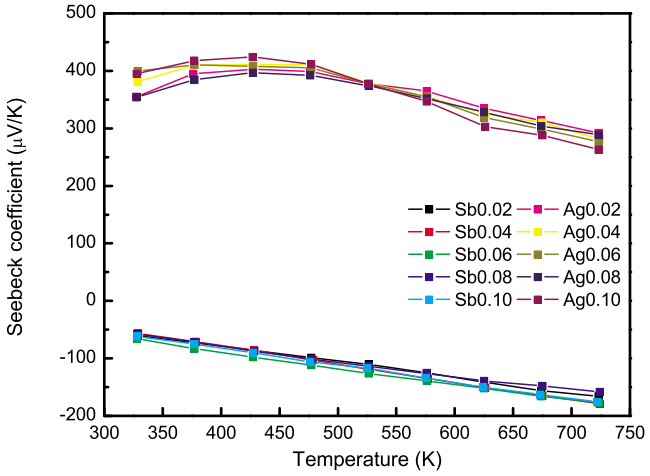

FIG. 4. (Color online) Temperature dependence of the Seebeck coefficient for the $Pb_{1-x}Ag_xTe$ and the $Pb_{1-x}Sb_xTe$ alloys.

due to small amounts of the elements. The composition of the second phase is hard to determine because the spectrum is disturbed by the matrix. The composition ratio of Pb to Te in the matrix is almost sustained in the Ag-doped compound, while decreased in the Sb-doped. This means that Sb is more soluble in PbTe than Ag, which is in accordance with the results of the lattice parameters. Based on the results of the microstructures, the chemical composition analysis, and the lattice parameters, it is concluded that the small amount of Ag or Sb, less than roughly x=0.02 in $Pb_{1-x}M_xTe$ (M=Ag or Sb), is substituted for Pb and the remained elements form the second phases. It is also noteworthy that most of Ag_5Te_3 is observed in the grain boundaries, whereas it is hard to conclude that most of Sb_2Te_3 is also in the grain boundaries. This can be understood based on the discrepancy in a solidification process between $Pb_{1-x}Ag_xTe$ and $Pb_{1-x}Sb_xTe$. Researches on the solidification process of the Sb-doped PbTe suggest that Sb_2Te_3 is formed from the eutectic reaction, liquid $\rightarrow$ PbTe+Sb_2Te_3, or the eutectoid reaction, $Pb_2Sb_6Te_{11} \rightarrow PbTe+Sb_2Te_3$.[21,22] From the these reaction, Sb_2Te_3 can be shaped in the forms of the lamellar, rod-like, globular, or acicular structure, which is depending on the feature of nucleation and growth.[21–23] However, Ag_5Te_3 is formed by the peritectic reaction, liquid+$Ag_2Te \rightarrow Ag_5Te_3$, where the liquid is interfacing with PbTe and Ag_5Te_3 is nucleated from Ag_2Te in the liquid.[24] Thus Ag_5Te_3 is placed in the grain boundaries whereas Sb_2Te_3 is placed in the matrix.

Figure 4 shows the temperature dependence of the Seebeck coefficient of the $Pb_{1-x}Ag_xTe$ and the $Pb_{1-x}Sb_xTe$ alloys. The Seebeck coefficient for the Ag-doped and the Sb-doped alloys shows the positive and the negative values, respectively, which mean that the major carriers of the Ag-doped alloys are holes, whereas those of the Sb-doped alloys are electrons. The n-type donor behavior by addition of Sb is consistent with the previous studies.[13] It is thought that Sb^{3+} substitute for Pb^{2+} in PbTe, and then a electron is produced, resulting n-type doping. This can be also adapted to the compound here, even though the second phase of Sb_2Te_3 exists. Because the Seebeck coefficient of Sb_2Te_3 is generally positive,[25] the negative Seebeck coefficient should come from the matrix PbTe. Moreover, Sb can be soluble in PbTe with small amount.[13] Thus it is concluded that some amount of Sb substitute for Pb, resulting in n-type doping, and the excess Sb is precipitated as the form of Sb_2Te_3, which is in accordance with the results of the lattice parameters and SEM. The p-type behavior of the Ag-doped samples can be

TABLE I. Chemical composition, carrier concentration, and mobility for $Pb_{1-x}M_xTe$ (M=Ag or Sb).

Composition	Chemical composition (at. %)			Carrier concentration (10^{18} cm^{-3})	Mobility (cm^2/V s)
	Pb	Te	Pb/Te		
$Pb_{0.98}Ag_{0.02}Te$	47.3	52.7	0.896	1.66	523
$Pb_{0.96}Ag_{0.04}Te$	47.3	52.7	0.896	1.37	465
$Pb_{0.94}Ag_{0.06}Te$	47.2	52.8	0.895	1.49	381
$Pb_{0.92}Ag_{0.08}Te$	47.1	52.9	0.891	1.27	287
$Pb_{0.90}Ag_{0.10}Te$	47.2	52.8	0.892	1.25	262
$Pb_{0.98}Sb_{0.02}Te$	47.8	52.2	0.914	2.67	2955
$Pb_{0.96}Sb_{0.04}Te$	47.2	52.8	0.895	8.47	841
$Pb_{0.94}Sb_{0.06}Te$	47.1	52.9	0.892	29.9	548
$Pb_{0.92}Sb_{0.08}Te$	46.5	53.5	0.868	171	110
$Pb_{0.90}Sb_{0.10}Te$	46.0	54.0	0.850	148	106

understood in a similar manner. It is known that the small amount of Ag can be soluble in PbTe, which is confirmed here by the results of the lattice parameters.[18,19] Thus, it is understood that Ag^{1+} substitute for Pb^{2+} and then a hole is produced, which in turns means p-type doping.[4,10–12] Ag_5Te_3 is usually described as $Ag_{5-x}Te_3$ and shows p-type transport behavior.[26] Thus both p-type elements of matrix and second phase may result in p-type transport for the Ag-doped samples, while it seems that the effect of the matrix phase is dominant than that of the second phase.

The carrier concentration and the mobility are estimated from the Hall coefficient measurement. The results are shown in Table I. Under the assumption of single-band conduction and a parabolic band model, the carrier concentration at room temperature is obtained from the Hall coefficient using the equation $R_H=1/ne$, where R_H is the Hall coefficient and n is the carrier concentration. The mobility can be calculated from the carrier concentration and the electrical resistivity. The values of the carrier concentration for the Sb-doped samples are considerably increased as the amount of the dopant is increased, whereas those of the Ag-doped are limitedly varied. However, the mobility is decreased with the dopant in both dopants. As mentioned in the result of the Seebeck coefficient, the doping effect of Sb on total Seebeck coefficient is dominant than that of the second phase. It is noteworthy that the Seebeck coefficient is largely dependent on the carrier concentration. Thus it may be concluded that the carrier concentration of the Sb-doped is increased due to the Sb-doping where Sb is substituted for Pb. Contrasting with the Sb-doping, it seems that the carrier concentration of the Ag-doped samples is little determined by the substitution of Ag for Pb. It is noteworthy that the solubility limit of Sb in PbTe is relatively larger than that of Ag, as mentioned previously. Thus the discrepancy in the dependence of the carrier concentration on the composition between the Sb-doped and the Ag-doped may be attributed to difference of the solubility limit. The decrease in the mobility may be attributed to the dopant scattering and the phase boundary scattering.

The temperature dependence of the Seebeck coefficient for the Sb-doped samples is of the semi-metallic behaviors, where the absolute value of the Seebeck coefficient is increased as the temperature increases, whereas that for the Ag-doped is of the degenerate semiconductor. The Seebeck coefficient for metals or degenerate semiconductors with the assumption of the parabolic band and the energy-independent scattering can be expressed as:[1]

$$S = \frac{8\pi^2 k_B^2 T}{3qh^2} m^* \left(\frac{\pi}{3n}\right)^{2/3}, \quad (1)$$

where k_B is the Boltzmann's constant, q is the carrier charge, h is the Plank's constant, and m^* is the effective mass of the carrier. It should be noted that Eq. (1) shows the Seebeck coefficient is highly dependent on the carrier concentration and decreased with the increasing the carrier concentration. The variation in the carrier concentration in the Ag-doped is relatively small, resulting in the negligible change in the Seebeck coefficient. However, the measured values of the Seebeck coefficient in the Sb-doped samples are almost unchanged as the carrier concentration significantly increases. In order to understand this peculiar behavior, the change in the effective mass with the Sb-doping may be considered. It is seen from Eq. (1) that as the amount of the Sb-doping is increased, the effective mass should be increased to maintain the Seebeck coefficient. From the measured carrier concentration and the Seebeck coefficient, the effective mass is estimated, which leads the value of m^* for $Pb_{0.90}Sb_{0.10}Te$ is larger about by a factor of 14.5 than that of $Pb_{0.98}Sb_{0.02}Te$. The increase in the effective mass means that the band structure near the conduction band minimum is significantly altered by doping, which is supported by the first-principles calculations.[27] The calculation shows that the Sb-doping in PbTe introduces the resonant states near the conduction band minimum.[27] The increase in the effective mass due to the resonant state near band edge is also observed in the Tl-doped PbTe.[6,27] In Tl–PbTe, the resonant states in the valence band edge are theoretically expected and confirmed experimentally.[6,27] As a result, the carrier concentration dependence of the Seebeck coefficient in Tl–PbTe does not follow Eq. (1) and the Seebeck coefficient is relatively enhanced.[6] To be similar with Tl–PbTe, it seems that the Seebeck coefficient of the Sb-doped samples may be considerably affected by the change in the effective mass.

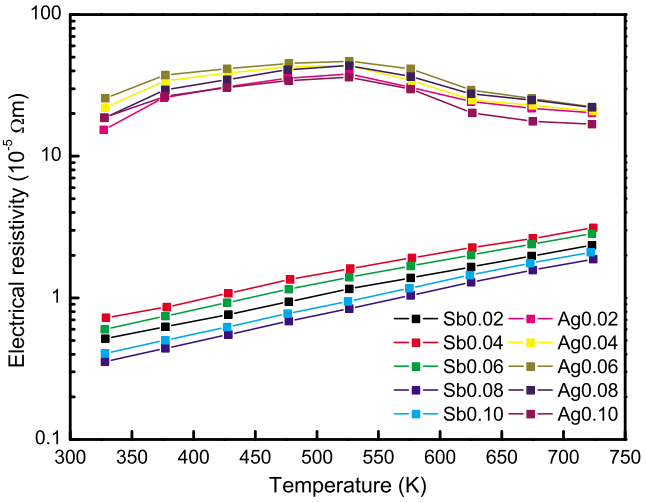

FIG. 5. (Color online) Temperature dependence of the electrical resistivity for the $Pb_{1-x}Ag_xTe$ and the $Pb_{1-x}Sb_xTe$ alloys.

Figure 5 shows the values of the electrical resistivity for $Pb_{1-x}Ag_xTe$ and $Pb_{1-x}Sb_xTe$ as a function of temperature. The electrical resistivity of the $Pb_{1-x}Ag_xTe$ alloys is increased from 323 to 523 K and then decreased after 523 K. This behavior of the electrical resistivity for the $Pb_{1-x}Ag_xTe$ alloys corresponds to that of the degenerate semiconductor. The temperature dependence of the Seebeck coefficient for $Pb_{1-x}Ag_xTe$ can be also understood as the behavior of the degenerate semiconductor. On the other hand, the electrical resistivity for the $Pb_{1-x}Sb_xTe$ alloys is increased in all temperature range, which is described as the semi-metallic characteristics. The results of the Seebeck coefficient for the Sb-doped samples confirm the same characteristics.

The temperature dependence of the thermal conductivity for the $Pb_{1-x}Ag_xTe$ and $Pb_{1-x}Sb_xTe$ alloys is shown in Fig. 6. The values of the heat capacity applied here for the

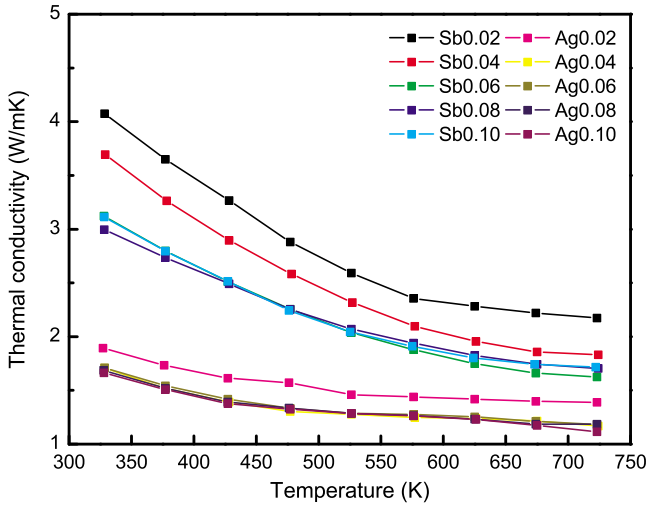

FIG. 6. (Color online) Temperature dependence of the thermal conductivity for the $Pb_{1-x}Ag_xTe$ and the $Pb_{1-x}Sb_xTe$ alloys.

samples are ranging from 0.15 to 0.17 J/g K in the temperature range of room temperature to 723 K and are limitedly varied with respect to the composition. The values of the thermal conductivity for the $Pb_{1-x}Ag_xTe$ alloys are about 1.8–1.6 W/mK at 323 K and decrease with increasing temperature, reaching about 1.6–1.3 W/mK at 723 K. On the other hand, the values of the thermal conductivity for the $Pb_{1-x}Sb_xTe$ alloys are about 4.1–3.0 W/mK at 323 K and decrease at elevated temperature, reaching about 2.2–1.8 W/mK at 723 K. The values of the thermal conductivity of the Ag-doped samples are lower than those of the Sb-doped samples. The reason for the lower thermal conductivity in the Ag-doped may be attributed to the higher electrical resistivity of the Ag-doped. The electrical contribution to the total thermal conductivity (κ_e) is usually calculated with Wiedemann–Frantz law, $\kappa_e = \sigma LT$, where L is the Lorentz number whose value is dependent the scattering mechanism, the concentration of electrons and holes, and so on.[28] The values of κ_e for the Ag-doped samples are approximately below 0.1 W/mK in the whole temperature range, whereas those of the Sb-doped are ranged from 0.5 to 2.3 W/mK. This is attributed to the lower electrical resistivity of the Sb-doped than that of the Ag-doped. The lattice thermal conductivity can be evaluated from the equation, $\kappa_{ph} = \kappa - \kappa_e$, where κ_{ph} is the lattice thermal conductivity and κ is the measured total thermal conductivity. The temperature dependence of the lattice thermal conductivity is shown in Fig. 7, in which the value of $L = 2.45 \times 10^{-8}$ V^2/K^2 is applied for the estimation of κ_e. The lattice thermal conductivity of the Ag-doped is little varied with the composition, whereas that of the Sb-doped is highly dependent on the amount of Sb. This may be related with the dopant scattering and the solubility limit of Ag and Sb in PbTe.

The temperature dependence of the ZT value is shown in Fig. 8. The ZT value for $Pb_{1-x}Ag_xTe$ and $Pb_{1-x}Sb_xTe$ is increased as the temperature is increased. The maximum ZT value of the $Pb_{1-x}Sb_xTe$ alloys shows 0.62 for x=0.1 at 723 K, which is mainly due to the low resistivity. The ZT value

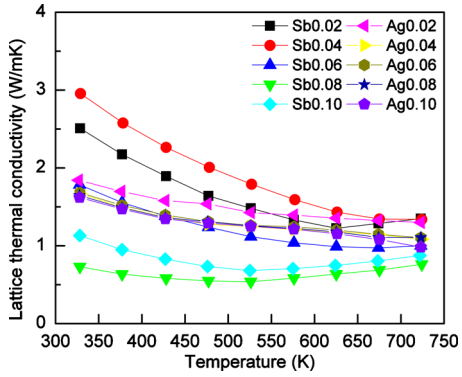

FIG. 7. (Color online) Temperature dependence of the lattice thermal conductivity for the $Pb_{1-x}Ag_xTe$ and the $Pb_{1-x}Sb_xTe$ alloys.

of the $Pb_{1-x}Ag_xTe$ alloys is about 0.1–0.2 at elevating temperature, which is due to the large electrical resistivity.

The thermoelectric properties of the Ag-doped and the Sb-doped PbTe compounds can be used to understand the thermoelectric properties of the LAST-m compounds. Especially, we're supposed to concentrate on the LAST-18 compound which is known as showing the best thermoelectric performance. It should be notable that the formula unit of LAST-18 is identical with the sum of $Pb_{0.9}Ag_{0.1}Te$ and $Pb_{0.9}Sb_{0.1}Te$. If the effect of interaction between Ag and Sb is negligible on the thermoelectric properties, the thermoelectric properties of the LAST-18 would be equal to or similar with summed properties of $Pb_{0.9}Ag_{0.1}Te$ and $Pb_{0.9}Sb_{0.1}Te$. We would like to call these properties here as the properties of the pseudo LAST-18. We would like to point the Seebeck coefficient out here, because the Seebeck coefficient is less affected by scattering than the other properties, especially at elevated temperature. Based on this behavior of the Seebeck coefficient, the value of the Seebeck coefficient can be often obtained from the electronic structure calculation and the results are quite well agreement with those of the experimental.[29] Thus we may have little considering on any interfacial problems raised when two systems are merged into a single system. When the contributions from the independent component to the total Seebeck coefficient (S_{tot}) are existed, the total Seebeck coefficient can be described as following,

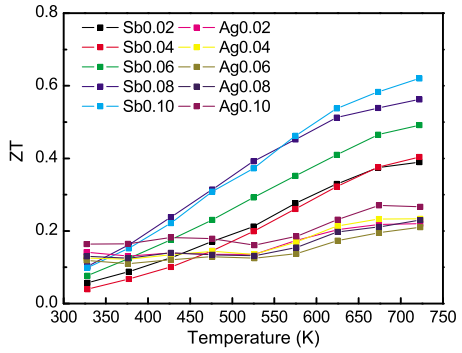

FIG. 8. (Color online) Temperature dependence of the ZT value for the $Pb_{1-x}Ag_xTe$ and the $Pb_{1-x}Sb_xTe$ alloys.

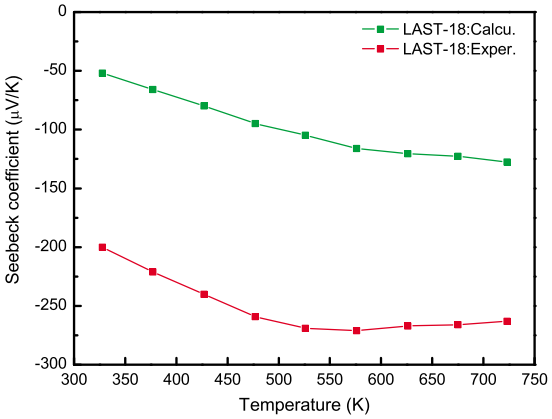

FIG. 9. (Color online) The Seebeck coefficient of the pseudo LAST-18 whose value was obtained from the sum of the Seebeck coefficient of $Pb_{0.9}Sb_{0.1}Te$ and $Pb_{0.9}Ag_{0.1}Te$ and the experimental LAST-18 alloys.

$$S_{tot} = \frac{\Sigma_i \sigma_i S_i}{\Sigma_i \sigma_i}, \tag{2}$$

where σ_i and S_i is the electrical conductivity and the Seebeck coefficient of the i component, respectively.[25] The calculated S_{tot} is plotted in Fig. 9 as a function of temperature. The experimental values are also introduced in Fig. 9. The experimental values refer to Ref. 17 where LAST-18 was fabricated with the same procedure used here. The absolute values of the Seebeck coefficient estimated with the values of the pseudo LAST-18 is much smaller than those of the experimental LAST-18. To explain this discrepancy, we may consider several possibilities such as the real amount of Ag and Sb in the Pb-sites in LAST-18, the presence of nanodots of the Ag-Sb compound, and the interaction between Ag and Sb in PbTe. When the amount of Ag in the Pb-sites is differ from that of Sb, the estimation of the Seebeck coefficient using the values of $Pb_{0.9}Ag_{0.1}Te$ and $Pb_{0.9}Sb_{0.1}Te$ should not be in accordance with that of LAST-18. Thus we may obtain S_{tot} with another combination between $Pb_{1-x}Ag_xTe$ and $Pb_{1-x}Sb_xTe$. However the increment of S_{tot} could not be achievable, because the Seebeck coefficient of the Ag-doped is positive and the absolute value of the Sb-doped is not larger than that of LAST-18. Thus it seems hard to say that the discrepancy is attributed the compositional variation. Even though the nanodots are clearly observed in several experiments for LAST-18 and known for reducing the thermal conductivity, the effect of the nanodots on the Seebeck coefficient is not clear.[8,9,15,16] On the other hand, the interaction of Ag and Sb is not easy to envisage. One expectation is found in the results of the first-principles calculation in which it was concluded that the distance between Ag and Sb in the PbTe lattice would be small.[30] However, the estimation using Eq. (2) implies that Ag and Sb are far from each other so that no interaction of Ag and Sb exists. Hence the discrepancy may be one of the indirect evidence that supports Ag and Sb are closely located in LAST-18 and interacting with each other. The interaction of Ag-Sb may be also supported by the results of the lattice parameters. The lattice parameters of LAST-m are decreased with increasing the amount of Ag and Sb, which means Ag and Sb are substitute for Pb. Moreover the nominal composition of LAST-m $(10<m<18)$ contains more Ag and Sb than the ternary system here. Even though the nanodots are presented in LAST-m, the results of the lattice parameters indicate that solubility of Ag and Sb in LAST-m is larger than that in the ternary system. Thus it seems that the interaction of Ag–Sb increases the solubility of Ag and Sb in PbTe and results in the enhanced thermoelectric properties. To sum up, the result of the Ag-doped and the Sb-doped may be one of supporting evidence that Ag and Sb do not separately contributed to the thermoelectric properties of LAST-18 but cooperate to enhance the thermoelectric properties of LAST-m.

IV. CONCLUSIONS

The polycrystalline $Pb_{1-x}Ag_xTe$ and $Pb_{1-x}Sb_xTe$ alloys were prepared by using a conventional melting method using a rocking furnace. The transport properties such as the Seebeck coefficient and the electrical conductivity for the $Pb_{1-x}Sb_xTe$ alloys exhibited the semi-metallic behavior with the n-type carriers. On the other hand, the transport properties for the $Pb_{1-x}Ag_xTe$ alloys showed the degenerate semiconductor behavior with the p-type carriers. The solubility limits of Sb and Ag in PbTe are estimated with the lattice parameters and the change in the carrier concentration. The change in the band structure near the conduction band edge is suggested by the carrier concentration dependence of the Seebeck coefficient, which leads the variation in the effective mass of the carrier. The highest ZT values for $Pb_{1-x}Sb_xTe$ and $Pb_{1-x}Ag_xTe$ were observed in $x=0.1$ for both compounds and reached 0.62 and 0.27 at 723 K, respectively. The larger ZT in the Sb-doped is mainly due to the lower electrical resistivity. The estimation of the Seebeck coefficient for the pseudo LAST-18 may support the evidence of the interaction between Ag and Sb in the LAST-18 compounds.

ACKNOWLEDGMENTS

This work was partly supported by Brain Korea 21 program. This work was also supported by the Energy Efficiency and Resources Program of the Korea Institute of Energy Technology Evaluation and Planning (KETEP) grant funded by the Ministry of Knowledge Economy, Republic of Korea (Grant No. 2008EID11P070000).

[1] G. J. Snyder and E. S. Toberer, Nature Mater. **7**, 105 (2008).
[2] B. C. Sales, Science **295**, 1248 (2002).
[3] V. Fano, in *CRC Handbook of Thermoelectrics*, edited by D. M. Rowe (CRC, Boca Raton, FL, 1995), p. 257.
[4] K. Ahn, C. Li, C. Uher, and M. G. Kanatzidis, Chem. Mater. **21**, 1361 (2009).
[5] J. Androulakis, C. H. Lin, H. J. Kong, C. Uher, C. I. Wu, T. Hogan, B. A. Cook, T. Caillat, K. M. Paraskevopoulos, and M. G. Kanatzidis, J. Am. Chem. Soc. **129**, 9780 (2007).
[6] J. P. Heremans, V. Jovovic, E. S. Toberer, A. Saramat, K. Kurosaki, A. Charoenphakdee, S. Yamanaka, and G. J. Snyder, Science **321**, 554 (2008).
[7] J. R. Sootsman, H. Kong, C. Uher, J. J. D'Angelo, C. I. Wu, T. P. Hogan, T. Caillat, and M. G. Kanatzidis, Angew. Chem., Int. Ed. **47**, 8618 (2008).
[8] K. F. Hsu, S. Loo, F. Guo, W. Chen, J. S. Dyck, C. Uher, T. Hogan, E. K. Polychroniadis, and M. G. Kanatzidis, Science **303**, 818 (2004).
[9] M. Zhou, J. F. Li, and T. Kita, J. Am. Chem. Soc. **130**, 4527 (2008).
[10] H. Kirby, J. Martin, A. Datta, L. Chen, and G. S. Nolas, *Materials and Devices for Thermal-to-Electric Energy Conversion*, MRS Symposia Pro-

ceedings No. 1166 (Materials Research Society, Pittsburgh, 2009), p. 71.
[11]J. Martin, L. Wang, L. Chen, and G. S. Nolas, Phys. Rev. B **79**, 115311 (2009).
[12]Y. Noda, M. Orihashi, and I. A. Nishida, Mater. Trans. **39**, 602 (1998).
[13]P. Zhu, Y. Imai, Y. Isoda, Y. Shinohara, X. Jia, and G. Zou, J. Phys.: Condens. Matter **17**, 7319 (2005).
[14]N. Chen, F. Gascoin, G. J. Snyder, E. Muller, G. Karpinski, and C. Stiewe, Appl. Phys. Lett. **87**, 171903 (2005).
[15]H. Lin, E. S. Božin, S. J. L. Billinge, E. Quarez, and M. G. Kanatzidis, Phys. Rev. B **72**, 174113 (2005).
[16]E. Quarez, K. F. Hsu, R. Pcionek, N. Frangis, E. K. Polychroniadis, and M. G. Kanatzidis, J. Am. Chem. Soc. **127**, 9177 (2005).
[17]H. S. Dow, M. W. Oh, S. D. Park, B. S. Kim, B. K. Min, H. W. Lee, and D. M. Wee, J. Appl. Phys. **105**, 113703 (2009).
[18]M. K. Sharov, Russ. J. Inorg. Chem. **54**, 33 (2009).
[19]M. K. Sharov, Inorg. Mater. **44**, 569 (2008).
[20]P. Zhu, Y. Imai, Y. Isoda, Y. Shinohara, X. Jia, and G. Zou, Mater. Trans. **46**, 1810 (2005).
[21]T. Ikeda, S. M. Haile, V. A. Ravi, H. Azizgolshani, F. Gascoin, and G. J. Snyder, Acta Mater. **55**, 1227 (2007).
[22]T. Ikeda, V. A. Ravi, and G. J. Snyder, Acta Mater. **57**, 666 (2009).
[23]W. F. Smith and J. Hashemi, *Foundations of Materials Science and Engineering*, 4th ed. (McGraw-Hill, New York, 2006), p. 332.
[24]F. Römermann and R. Blachnik, J. Alloys Compd. **280**, 147 (1998).
[25]G. S. Nolas, J. Sharp, and J. Goldsmid, *Thermoelectrics: Basic Principles and New Materials Developments* (Springer, Berlin, 2001), pp. 43–122.
[26]W. Freyland and O. Madelung, *Physics of Non-Tetrahedrally Bonded Elements and Binary Compounds I*, Landolt-Börnstein New Series, Group III, Semiconductors Vol. 17 (Springer-Verlag, Berlin, 1996), p. 141.
[27]S. Ahmad, S. D. Mahanti, K. Hoang, and M. G. Kanatzidis, Phys. Rev. B **74**, 155205 (2006).
[28]J. E. Parrott and A. D. Stuckes, *Thermal Conductivity of Solids* (Pion, London, 1975), pp. 44–89.
[29]M. W. Oh, D. M. Wee, S. D. Park, B. S. Kim, and H. W. Lee, Phys. Rev. B **77**, 165119 (2008).
[30]H. Hazama, U. Mizutani, and R. Asahi, Phys. Rev. B **73**, 115108 (2006).